Neoplasia • Vol. 9, No. 11, November 2007, pp. 979–986 979

www.neoplasia.com

Stromal Metalloproteinase-9 Is Essential to Angiogenesis and Progressive Growth of Orthotopic Human Pancreatic Cancer in Parabiont Nude Mice[1]

Toru Nakamura, Toshio Kuwai, Jang-Seong Kim, Dominic Fan, Sun-Jin Kim and Isaiah J. Fidler

Department of Cancer Biology, The University of Texas M. D. Anderson Cancer Center, Houston, TX, USA

Abstract

We determined whether host matrix metalloproteinase (MMP) 9 is essential to angiogenesis and to the growth of L3.6pl human pancreatic cancer cells implanted into the pancreas of wild-type (*MMP-9*$^{+/+}$) and knockout (*MMP-9*$^{-/-}$) nude mice. Four weeks after tumor cell injection, pancreatic tumors in *MMP-9*$^{+/+}$ mice were large, had many blood vessels, and contained many macrophages expressing MMP-9. In contrast, pancreatic tumors in *MMP-9*$^{-/-}$ mice were significantly smaller, had few blood vessels, and had few macrophages. Next, we parabiosed *MMP-9*$^{+/+}$ mice with *MMP-9*$^{+/+}$ mice, *MMP-9*$^{-/-}$ mice with *MMP-9*$^{-/-}$ mice, and *MMP-9*$^{+/+}$ mice with *MMP-9*$^{-/-}$ mice. Two weeks after parabiosis, we implanted L3.6pl cells into the pancreas of the recipient mouse in each pair. Four weeks later, the mice were necropsied. The parabiosis experiment revealed a direct correlation between intratumoral MMP-9$^{+/+}$ expressing macrophages, angiogenesis, and progressive tumor growth. Because the expression of *MMP-9* by L3.6pl tumor cells was similar in all parabionts, the data clearly demonstrate a major role for host-derived MMP-9 in angiogenesis and in the growth of human pancreatic cancer in the pancreas of nude mice.

Neoplasia (2007) **9,** 979–986

Keywords: MMP-9, parabiosis, pancreatic cancer, angiogenesis, orthotopic model.

Introduction

After the initial transformation and growth of malignant cells, tumors must recruit a new vasculature to expand beyond 1 mm in diameter. This recruitment is accomplished by the synthesis and secretion of several proangiogenic factors by tumor cells and infiltrating host cells, leading to the development of a capillary network that is connected to surrounding host tissues [1,2]. The infiltration of leukocytes into tumors is known to promote angiogenesis and progressive growth of lesions [3–5]. Histopathological data obtained from multiple clinical cancer specimens reveal that the higher is the density of leukocyte infiltration into tumors, the worse is the disease outcome [6–13]. For example, chronic pancreatitis is known to increase the risk of developing pancreatic cancer [14–16], and this risk is associated with the presence of inflammatory cells [17–19].

To produce a new vasculature, endothelial cells must migrate, divide, and form tubes [20,21]. Proteolysis of the extracellular matrix [22,23] facilitates migration and releases stored angiogenic signaling molecules from the extracellular matrix [24,25]. High levels of matrix metalloproteinase (MMP) 9 in tissues are associated with active neovascularization [22–25]. Studies in mice genetically modified to lack MMP-9 expression [24–27] have shown that MMP-9 expressed by host inflammatory–stromal cells contributes to angiogenic switch that occurs during carcinogenesis [24,25,28]. Human pancreatic cancers express both MMP-2 and MMP-9 [29–31], and increased expression of these MMPs is associated with invasive and metastatic potential [30,31]. Whether the MMP-9 produced by stromal cells within these tumors plays a major role in angiogenesis and tumor expression is unclear.

Recently, we have reported that host MMP-9 expression contributes to angiogenesis and the progressive growth of human ovarian cancer cells implanted into the peritoneal cavities of female nude mice that lacked the gene for MMP-9 (*MMP-9*$^{-/-}$) or were wild-type for MMP-9 (*MMP-9*$^{+/+}$) [28]. Intraperitoneal injection of nucleated spleen cells from young *MMP-9*$^{+/+}$ nude mice into *MMP-9*$^{-/-}$ nude mice promoted the growth of human ovarian cancer cells implanted into the peritoneal cavity, indicating that host-derived MMP-9 (most likely in tumor-infiltrating macrophages) plays a major role in progressive tumor growth [28]. To determine whether host-derived MMP-9 is also essential to angiogenesis and the progressive growth of orthotopically implanted human pancreatic cancer in nude mice, we used the parabiosis method to reconstitute *MMP-9*$^{-/-}$ mice with *MMP-9*$^{+/+}$ circulating cells. The data clearly show that infiltration of *MMP-9*$^{+/+}$ macrophages into

Abbreviations: GFP, green fluorescent protein; MMP, matrix metalloproteinase; MVD, microvessel density; PBS, phosphate-buffered saline; PCR, polymerase chain reaction; PECAM-1, platelet–endothelial cell adhesion molecule-1

Address all correspondence to: Isaiah J. Fidler, DVM, PhD, Department of Cancer Biology, The University of Texas M. D. Anderson Cancer Center, Unit 173, PO Box 301429, Houston, TX 77230-1429. E-mail: ifidler@mdanderson.org

[1]This research was supported, in part, by Cancer Center Support Core grant CA16672 and SPORE in Prostate Cancer grant CA90270 from the National Cancer Institute, National Institutes of Health.

Received 15 August 2007; Revised 5 September 2007; Accepted 7 September 2007.

DOI 10.1593/neo.07742

orthotopic human pancreatic tumors correlates with angiogenesis and the progressive growth of tumors.

Materials and Methods

Human Pancreatic Cancer Cell Line

Human pancreatic cancer L3.6pl [32] cells were maintained in Eagle's minimal essential medium supplemented with 10% fetal bovine serum, sodium pyruvate, nonessential amino acids, L-glutamine, a two-fold vitamin solution (Life Technologies, Inc., Grand Island, NY), and a penicillin–streptomycin mixture (Flow Laboratories, Rockville, MD). Adherent monolayer cultures were maintained on plastic and incubated at 37°C in a mixture of 5% CO_2 and 95% air. The cultures were free of *Mycoplasma* and the following pathogenic murine viruses: reovirus type 3, pneumonia virus, K virus, Theiler's encephalitis virus, Sendai virus, minute virus, mouse adenovirus, mouse hepatitis virus, lymphocytic choriomeningitis virus, ectromelia virus, and lactate dehydrogenase virus (assayed by the Research Animal Diagnostic Laboratory, University of Missouri, Columbia, MO). The cultures were maintained for no longer than 12 weeks after recovery from frozen stock.

Animals

Athymic BALB/c nude mice with wild-type *MMP-9* genes (MMP-$9^{+/+}$) were purchased from the Animal Production Area of the National Cancer Institute's Frederick Cancer Research Facility (Frederick, MD). Mice lacking an intact *MMP-9* gene were originally developed through homologous recombination in mice with a 129/CD1 genetic background [26]. We generated the *MMP-*$9^{-/-}$ female nude mice used in the current study by breeding *MMP-*$9^{-/-}$ 129/CD1 mice with *MMP-*$9^{+/+}$ female nude mice for eight generations [28]. The nude mice were housed under pathogen-free conditions and used for all studies when they were 8 to 12 weeks old. Mice used for parabiosis were age-matched. Animals were maintained according to institutional regulations and in facilities approved by the American Association for Accreditation of Laboratory Animal Care, in accordance with current regulations and standards of the US Department of Agriculture, Department of Health and Human Services, and the National Institutes of Health.

Genotyping of Mouse MMP-9 By Polymerase Chain Reaction Analysis

The genotypes of the mice were determined by using polymerase chain reaction (PCR) analysis [27]. Tails or spleens were digested in a buffer containing proteinase K and extracted twice by using phenol. DNA was precipitated and resuspended in TE buffer (10 mM Tris base, 1 mM EDTA, pH 7.5) containing RNase A. Three hundred nanograms of DNA was used in a 50-μl PCR. We used two pairs of PCR primers in the same reaction (one for *MMP-9* and one for neomycin), which were used to replace most of exon 2 and all of intron 2 on the *MMP-9* gene in *MMP-*$9^{-/-}$ mice [27]. The sequences of the *MMP-9* exon 2 forward and reverse primers were 5′-GCATACTTGTACCGCTATGG-3′ and 5′-TGTGATGTTATGATGGTCCC-3′, respectively. These primers yielded a 224-bp product that was only present in the unaltered allele (most of exon 2 and all of intron 2 are deleted in the knockout allele). The sequences of neomycin PCR primers were 5′-ATGATTGAACAAGATGGATTGCAC-3′ and 5′-TTCGTCCAGATCATCCTGATCGAC-3′, respectively. These primers yielded a 479-bp product that was only present in the knockout allele. PCR took place in a Mastercycler gradient 5331 (Eppendorf, Hamburg, Germany) at 98°C for 20 seconds, 65°C for 30 seconds, and 68°C for 30 seconds, for 35 cycles. All PCR products were separated by electrophoresis on 2% agarose gels.

Orthotopic Model for Pancreatic Cancer

To produce pancreatic tumors, L3.6pl cells were harvested from subconfluent cultures by brief exposure to a phosphate-buffered saline (PBS) solution containing 0.25% trypsin and 0.02% EDTA. Trypsinization was stopped with a medium containing 10% fetal bovine serum, and the cells were washed once in serum-free medium and resuspended in Hank's balanced salt solution. Only single-cell suspensions of > 90% viability (trypan blue exclusion) were used for injection into the pancreas.

The mice were anesthetized by an intramuscular injection of pentobarbital (0.5 mg/kg). Abdominal skin was cleaned with 70% alcohol, and a small left abdominal flank incision was made. The spleen was exteriorized, and the pancreas was identified in a region just beneath the spleen. A 30-gauge needle was inserted into the pancreas, and tumor cells (1×10^6 per 50 μl of Hanks' balanced salt solution) were injected subcapsularly [32]. The abdominal wound was closed in one layer with wound clips (Auto-clip; Clay Adams, Parsippany, NJ). The animals tolerated the surgical procedure well, and no procedure-related deaths occurred.

After 4 weeks, the mice were euthanized and pancreatic tumors were harvested. A portion was fixed in formalin and another portion was immediately embedded in ornithine carbamyl transferase compound (Miles, Elkhart, IN), rapidly frozen in liquid nitrogen, and stored at −80°C. Comparative experiments were performed concurrently.

Immunohistochemical Analysis and Quantitation of Microvessel Density

Pancreatic tumors were harvested at autopsy and processed for immunostaining as previously described [32] using the following antibodies: rat polyclonal antibody F4/80, which recognizes the mouse macrophage-specific antigen F4/80 (1:100 dilution, MCAP497; Serotec, Inc., Raleigh, NC); anti–human MMP-9 rabbit polyclonal antibody (1:100 dilution, AB13458; Chemicon, Temecula, CA); anti–CD31/platelet–endothelial cell adhesion molecule-1 (PECAM-1) monoclonal antibody, which recognizes PECAM-1 on endothelial cells (1:400 dilution, 25 μg/ml, mouse-specific; BD Pharmingen, San Diego, CA); and appropriate horseradish peroxidase–conjugated secondary antibodies (Jackson

ImmunoResearch Laboratories, Inc., West Grove, PA). Negative controls were stained with nonspecific immunoglobulin (Ig) G and appropriate horseradish peroxidase–conjugated secondary antibody. All sections were counterstained with Gill's hematoxylin. Immunostained tumor sections were examined by bright-field microscopy. For the quantification of microvessel density (MVD) or macrophage infiltration, 10 random 0.159-mm^2 fields at ×100 magnification were captured, and CD31-positive or F4/80–positive cells were counted [33]. Images were digitized by using a Sony 3CD color video camera (Sony Corp., Tokyo, Japan) and a personal computer equipped with Optimas image analysis software (Optimas Corp., Bothell, WA).

Immunofluorescence Double Staining for F4/80 and MMP-9

Frozen specimens of human pancreatic carcinoma cells growing in the pancreata of nude mice were cut into 4-μm sections, mounted on positively charged slides, and stored at −80°C. Tissue sections were fixed in cold acetone for 10 minutes and then washed three times with PBS for 3 minutes each. The slides were placed in a humidified chamber and incubated with protein-blocking solution (4% fish gelatin in PBS) for 20 minutes at room temperature. The slides were then incubated overnight at 4°C with goat polyclonal anti–mouse MMP-9 antibody (AF909; R&D Systems, Minneapolis, MN) at a 1:60 dilution (17 μg/ml). Next, the slides were rinsed three times with PBS, incubated for 10 minutes in protein-blocking solution, and then incubated for 1 hour at room temperature with Alexa 488–conjugated anti-goat secondary antibody at 1:400 dilution (Molecular Probes, Inc., Eugene, OR). From this step onward, the slides were protected from light. They were rinsed three times in PBS and incubated for 20 minutes at room temperature with protein-blocking solution (5% normal horse serum and 1% normal goat serum in PBS). They were then incubated overnight at 4°C with a 1:100 dilution of F4/80 (10 μg/ml MCAP497; Serotec, Inc.). The slides were rinsed three times with PBS and incubated for 10 minutes in protein-blocking solution. They were then incubated for 1 hour at room temperature with a 1:400 dilution of Alexa 594–conjugated anti-rat secondary antibody (Molecular Probes, Inc.). They were then rinsed three times in PBS and counterstained with Hoechst 3342 (100 μg/ml in PBS). The slides were then rinsed three times with PBS, and a mounting medium was placed on each sample and covered with a glass cover slip (Fischer Scientific, Pittsburgh, PA). The mounting medium consisted of 90% glycerol, 10% PBS, and 0.1 M propyl gallate. The concentrations of stock antibody used were adjusted to 1.0 mg/ml. IgG antibodies were selected and matched to secondary antibodies such as rat (012-000-003; Jackson ImmunoResearch Laboratories, Inc.), rabbit (011-000-003; Jackson ImmunoResearch Laboratories, Inc.), and mouse (015-000-003; Jackson ImmunoResearch Laboratories, Inc.) IgG.

Immunofluorescence microscopy was conducted using a Zeiss Axioplan fluorescence microscope (Carl Zeiss, Inc., Thornwood, NY). Images were captured with a cooled C5810 camera (Hamamatsu Photonics KK, Bridgewater, NJ) using Optimas software (Media Cybernetics, Silver Spring, MD) run on a Dell personal computer (Dell, Round Rock, TX). MMP-9 staining was identified by red fluorescence, and F4/80 staining was detected by green fluorescence. Colocalization of MMP-9 and F4/80 was detected by yellow fluorescence.

Parabiosis

The parabiosis mouse model can be used as a powerful tool to study sequential biologic events [34,35]. We tested whether circulating cells (including lymphoreticular cells) from a *MMP-9*$^{+/+}$ nude mouse populating an *MMP-9*$^{-/-}$ nude mouse stimulate the growth of L3.6pl cells injected into the pancreas of the *MMP-9*$^{-/-}$ nude mouse. Parabiosis was performed according to the technique originally described by Eichwald et al. [33], with modifications. *MMP-9*$^{-/-}$ nude mice and normal nude mice (*MMP-9*$^{+/+}$) were anesthetized with pentobarbital. An incision through the skin and panniculus was made from the hind leg to the front leg on each partner. A subpannicular space extending approximately 15 mm was created by blunt dissection. The latissimus dorsi and abdominal external oblique muscles on each mouse were split. The peritoneal cavities were not penetrated. The muscles were sutured together with absorbable sutures. The skin and panniculus of the two mice were sutured together continuously with monofilament suture material. To improve postsurgery wound healing and to prevent the separation of parabionts, a flexible cohesive veterinarian bandage (1 in. width, cat no. COFLEX1; Med-Vet International, Mettawa, IL) was wrapped around the two parabionts. The parabionts were placed in a cage (1 pair/cage) for a 2-week recovery period before the experiments. The parabiosed mice recovered exceptionally well from the procedure. To prevent pain, we administered aspirin (100–120 mg/kg, po, twice daily) for 2 days, as prescribed by the Institutional Animal Care and Use Committee's Analgesia Standard Operating Procedures. Common circulation was usually established by 7 to 10 days after parabiosis. Viable anastomoses of the parabiosis system were determined by microscopic examination of cross-circulated green fluorescent protein (GFP) erythrocytes in the normal mouse (GFP-negative) and in non-GFP erythrocytes in a GFP parabiont (data not shown).

Statistical Analysis

Mann-Whitney *U* test was used to compare tumor weight, the number of macrophage infiltrations, and MVD (CD31/PECAM-1) in *MMP-9*$^{+/+}$ and *MMP-9*$^{-/-}$ nude mice. All statistical tests were two-sided, and the *P* value cutoff for statistical significance was .01.

Results

Human Pancreatic Cancer Cell Growth in the Pancreas of MMP-9 *Knockout Mice*

In the first set of experiments, we injected L3.6pl cells into the pancreas of six *MMP-9*$^{+/+}$ mice and six *MMP-9*$^{-/-}$ nude mice (the available number of animals). Pancreatic tumors

developed in all six *MMP-9*$^{+/+}$ nude mice, but only three of the *MMP-9*$^{-/-}$ nude mice developed tumors that were significantly smaller than those in *MMP-9*$^{+/+}$ mice ($P < .01$). The median weight of the L3.6pl tumors in *MMP-9*$^{+/+}$ nude mice was 0.93 g (interquartile range, 0.24–1.76 g), whereas it was 0.1 g (interquartile range, 0–0.28 g) in *MMP-9*$^{-/-}$ nude mice. Thus, disruption of the *MMP-9* gene in recipient mice decreased tumorigenicity and the size of human pancreatic cancer cells in the pancreas.

Effect of Tumor Cell–Derived MMP-9 on MMP-9$^{-/-}$ *Mice*

Because both human pancreatic cancer cells and cells from *MMP-9*$^{+/+}$ mice produced MMP-9, we determined whether the difference in tumor incidence between *MMP-9*$^{+/+}$ and *MMP-9*$^{-/-}$ mice was associated with MMP-9 produced by mouse cells or human cancer cells. The *in vivo* expression level of MMP-9 in tumor cells growing in mice was determined by immunohistochemical analysis using an anti–human MMP-9 antibody. As shown in Figure 1, the level of MMP-9 produced by L3.6pl cells was similar in *MMP-9*$^{-/-}$ and *MMP-9*$^{+/+}$ nude mice.

Macrophage Infiltration of Pancreatic Tumors Growing in MMP-9$^{+/+}$ *and* MMP-9$^{-/-}$ *Nude Mice*

MMP-9 is expressed in macrophages, which are a major component of lymphoreticular cells that infiltrate tumors [34]. We used immunohistochemistry to characterize the tumor-infiltrating macrophages in L3.6pl pancreatic tumors (Figure 1). Specific staining for macrophages with the F4/80 antibody revealed the presence of macrophages throughout the L3.6pl tumors in *MMP-9*$^{+/+}$ nude mice (median number of macrophages per field = 155; range, 117–277). In contrast, L3.6pl tumors in *MMP-9*$^{-/-}$ mice contained fewer macrophages (median number of macrophages per field = 54; range, 42–79).

Angiogenesis in Pancreatic Tumors in MMP-9$^{-/-}$ *and* MMP-9$^{+/+}$ *Nude Mice*

Next, we determined whether macrophage infiltration into human pancreatic tumors was associated with the formation of blood vessels [36]. MVD in L3.6pl tumors in the pancreas of *MMP-9*$^{-/-}$ and *MMP-9*$^{+/+}$ nude mice was determined by

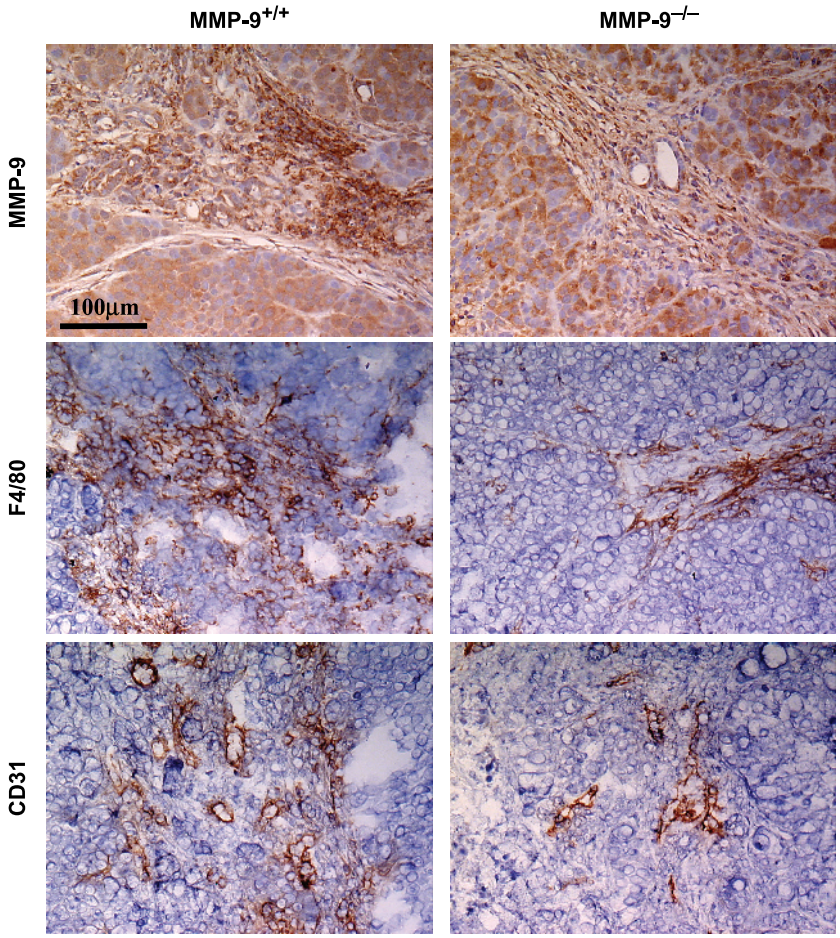

Figure 1. *Immunohistochemical analysis of MMP-9, F4/80, and CD31/PECAM-1. L3.6pl human pancreatic cancer cells were injected into the pancreata of MMP-9*$^{+/+}$ *and MMP-9*$^{-/-}$ *nude mice. After 4 weeks, pancreatic tumors were processed for immunohistochemical analysis. Tumor sections were immunostained with an anti–human MMP-9 antibody to detect MMP-9 expressed by human L3.6pl tumor cells. Macrophage infiltration was determined by immunostaining with an anti–F4/80 antibody. Blood vessels in the tumors were visualized and counted after immunostaining with an anti-CD31 antibody. The staining patterns shown are representative of those observed for at least 10 random fields. All sections were counterstained with Gill's hematoxylin (blue). Brown indicates specific antibody reactivity.*

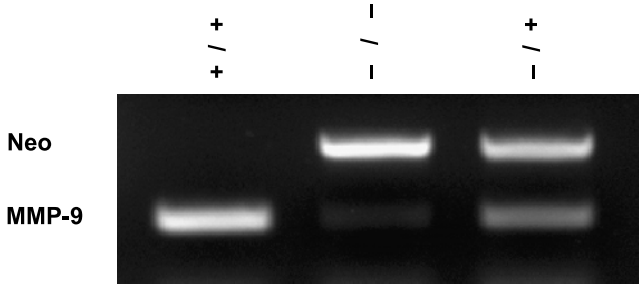

Figure 2. *Genotyping of mouse* MMP-9 *in spleen cells was performed by PCR. DNA was derived from recipient mouse spleen cells in each group. (+/+) DNA from recipient* MMP-$9^{+/+}$ *mouse parabiosed with* MMP-$9^{+/+}$ *nude mouse. (−/−) DNA from recipient* MMP-$9^{-/-}$ *mouse parabiosed with MMP-*$9^{-/-}$ *mouse. (+/−) DNA from recipient* MMP-$9^{-/-}$ *mouse parabiosed with MMP-*$9^{+/+}$ *mouse. Neomycin (Neo) was used to replace most of exon 2 and all of intron 2 of the* MMP-9 *gene in* MMP-$9^{-/-}$ *mice.* MMP-9 *(a 224-bp product) is only present in the unaltered allele, and Neo (a 479-bp product) is only present in the knockout allele.*

staining for CD31 (Figure 1). In *MMP-*$9^{+/+}$ nude mice, L3.6pl tumors were highly vascularized, with a median of 71 microvessels per field (range, 54–96), whereas the median number of microvessels per field was 27 (range, 21–33) in *MMP-*$9^{-/-}$ nude mice ($P < .001$).

Tumorigenicity in Reconstituted MMP-9−/− *Parabiotic Mice*

The presence of *MMP-9*–expressing cells in the spleens of *MMP-*$9^{-/-}$ nude mice reconstituted by parabiosis into MMP-$9^{+/+}$ nude mice was confirmed by PCR from DNA extraction of the spleens (Figure 2). Three parabiotic groups were used, as shown in Table 1. The first group consisted of *MMP-*$9^{+/+}$ nude mice parabiosed with *MMP-*$9^{+/+}$ nude mice (positive control group); the second group consisted of *MMP-*$9^{-/-}$ nude mice parabiosed with *MMP-*$9^{-/-}$ nude mice (negative control group); and the third group consisted of *MMP-*$9^{-/-}$ nude mice parabiosed with *MMP-*$9^{+/+}$ nude mice (MMP-9–reconstituted group). Two weeks after the parabiosis procedure, L3.6pl cells were injected into the pancreas of one mouse in each pair (recipient mouse). Parabiont hosts were not injected. The tumorigenicity of the L3.6pl cells was determined 4 weeks after injection. As shown in Table 1, all injected mice in the first group (*MMP-*$9^{+/+}$ with *MMP-*$9^{+/+}$) developed pancreatic tumors (median tumor weight = 1.0 g), whereas only 5 of 10 injected mice in the second group (*MMP-*$9^{-/-}$ with *MMP-*$9^{-/-}$) developed pancreatic tumors, which were much smaller (median weight = 0.1 g) ($P < .001$). This result was consistent with those of the first set of studies shown, as discussed previously. All of the injected mice in the third group (*MMP-*$9^{-/-}$ with *MMP-*$9^{+/+}$) developed pancreatic tumors that were larger (median weight = 0.7 g) than those of the second group ($P < .001$). These results indicate that reconstitution of *MMP-*$9^{-/-}$ nude mice with *MMP-*$9^{+/+}$ cells (but not with *MMP-*$9^{-/-}$ cells) increases the growth of L3.6pl pancreatic tumors. Moreover, the MVD and macrophage infiltration of pancreatic tumors were significantly higher in the third group than in the second group ($P < .001$) (Table 1).

MMP-9 Production By Tumor-Infiltrating Macrophages

Next, we examined whether MMP-9 expression in tumor-infiltrating macrophages was associated with angiogenesis and the progressive growth of orthotopic human pancreatic cancers in nude mice. Pancreatic tumors from the three groups of parabiotic mice (Table 1) were resected and processed for immunohistochemical analysis. MMP-9–expressing mouse cells were detected with an anti–MMP-9 antibody specific for murine MMP-9 and visualized by red fluorescent signals. Tumor-infiltrating macrophages were detected with an antibody against the macrophage-specific marker F4/80 and were visualized by green fluorescent signals. Colocalization of the two antibodies yielded a yellow fluorescent signal. Pancreatic tumors in *MMP-*$9^{+/+}$ with *MMP-*$9^{+/+}$ parabionts contained F4/80–positive macrophages that expressed MMP-9 (Figure 3). Tumors in *MMP-*$9^{-/-}$ with MMP-$9^{-/-}$ parabionts contained F4/80–positive macrophages that did not express MMP-9. Tumors from *MMP-*$9^{-/-}$ nude mice that were parabiosed with *MMP-*$9^{+/+}$ nude mice contained a few macrophages that expressed MMP-9 (Figure 3). These data confirm that the increased angiogenesis and growth of human pancreatic tumors in the pancreas of *MMP-*$9^{-/-}$ nude mice reconstituted with *MMP-*$9^{+/+}$ cells were associated with the infiltration of MMP-9–expressing macrophages.

Discussion

Our results demonstrate that MMP-9 produced by circulating macrophages plays an important role in the angiogenesis and growth of human pancreatic cancer cells implanted into the pancreas of nude mice. In *MMP-*$9^{+/+}$ mice, orthotopically injected L3.6pl cells produced highly vascularized and rapidly growing tumors, whereas in *MMP-*$9^{-/-}$ mice, the tumor

Table 1. Effect of Parabiosis Reconstitution with *MMP-*$9^{+/+}$ and *MMP-*$9^{-/-}$ Nude Mice on the Growth of Human Pancreatic Cells in *MMP-*$9^{-/-}$ Nude Mice.

Nude Mice		Pancreatic Tumors in Injected Mice			Macrophage Infiltration		MVD	
Injected (Recipient)	Parabiont (Donor)	Incidence	Tumor Weight (g) [Median (Range)]	*P**	Median Number/Field (Range)	*P**	Median Number/Field (Range)	*P**
MMP-$9^{+/+}$	*MMP-*$9^{+/+}$	10/10	1.0 (0.5–1.9)	< .001	152 (90–207)	< .001	68 (55–91)	< .001
MMP-$9^{-/-}$	*MMP-*$9^{-/-}$	5/10	0.1 (0.0–0.3)		55 (32–80)		25 (19–40)	
MMP-$9^{-/-}$	*MMP-*$9^{+/+}$	10/10	0.7 (0.4–1.3)		108 (80–179)		58 (42–73)	

Nude mice were parabiosed 2 weeks before L3.6pl human pancreatic cancer cells were injected into the pancreas of the recipient mouse. The parabiosed mice were killed 4 weeks later.

*Mann-Whitney *U* test (one field = 0.159 mm^2 at ×100 magnification).

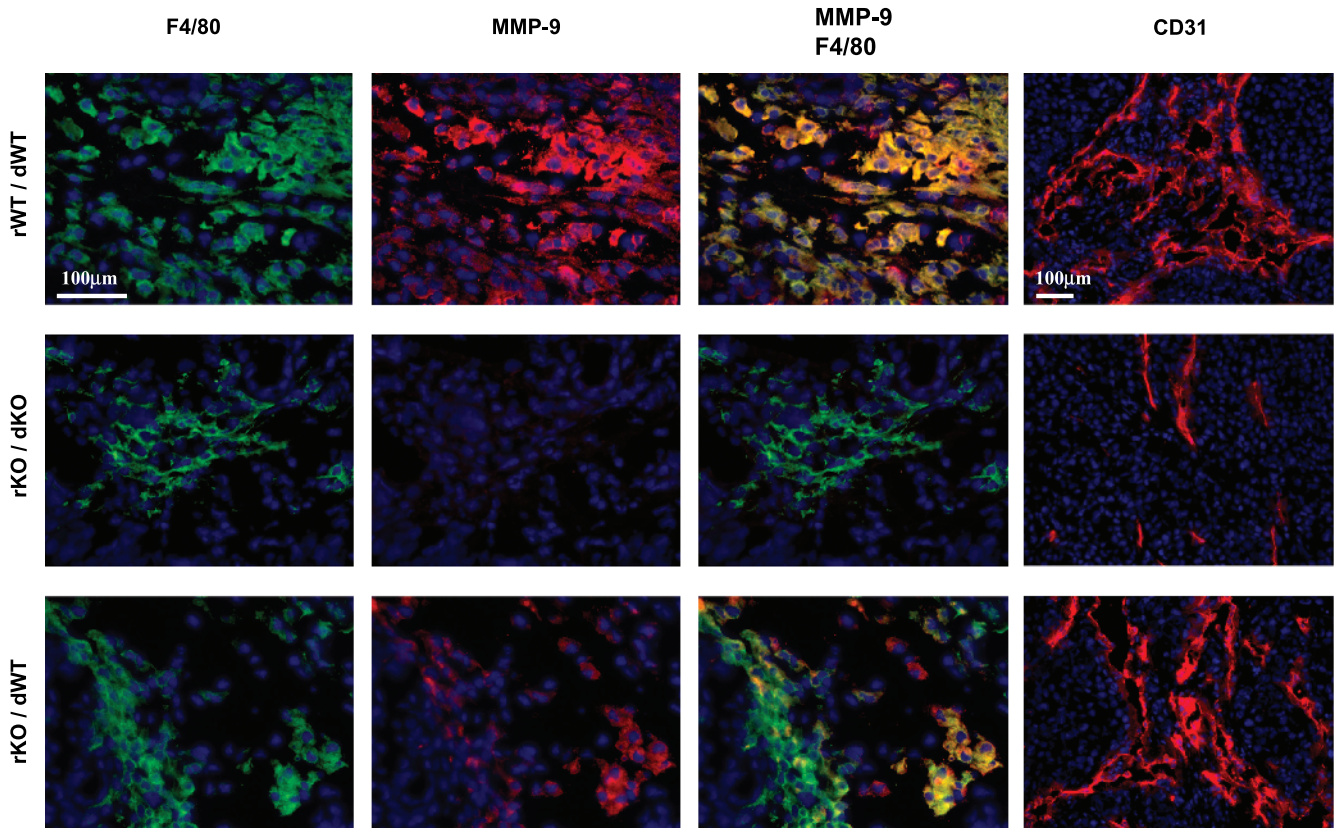

Figure 3. *Double immunofluorescent staining for macrophage marker F4/80 and mouse MMP-9 in L3.6pl pancreatic tumors. Nude mice were parabiosed 2 weeks before 1 × 10^6 L3.6pl cells were injected into the pancreas of the recipient mouse. Four weeks later, pancreatic tumors were processed for immunofluorescent analysis. rWT/dWT, a representative of the pancreatic tumor from an MMP-$9^{+/+}$ nude mouse parabiosed with an MMP-$9^{+/+}$ nude mouse (positive control). rKO/dKO, the pancreatic tumor from an MMP-$9^{-/-}$ nude mouse parabiosed with an MMP-$9^{-/-}$ nude mouse (negative control). rKO/dWT, the pancreatic tumor from an MMP-$9^{-/-}$ nude mouse parabiosed with an MMP-$9^{+/+}$ nude mouse (host MMP-9 reconstitution). Macrophages were detected by using macrophage marker F4/80 antibodies (green), and the host MMP-9 was detected by using anti–mouse-specific MMP-9 antibodies (red). Double-immunofluorescent staining for F4/80 and mouse MMP-9 (yellow) demonstrated that only the macrophages of wild-type mice expressed MMP-9. Blood vessels in the tumors were detected by an anti-CD31 antibody (red).*

cells produced fewer, smaller tumors with low MVD. The decrease in angiogenesis in mice that lacked MMP-9 expression was associated with a decrease in macrophage infiltration into pancreatic tumors. When the mice that lacked MMP-9 expression were parabiosed with MMP-$9^{+/+}$ mice, the tumorigenicity of pancreatic tumors increased, suggesting that tumor-infiltrating macrophages that produce MMP-9 played a major role in the angiogenesis and growth of pancreatic tumors.

Expression of MMP-9 enhances carcinogenesis in pancreatic islets and skin epithelium by triggering angiogenic switch [24,25]. In a mouse model of skin carcinogenesis, MMP-9 was predominantly expressed in inflammatory cells rather than in oncogene-positive neoplastic cells, suggesting that inflammatory cells are the critical suppliers of MMP-9 in this pathway of carcinogenesis [23]. Specifically, Coussens et al. [37] demonstrated that mast cells that are prevalent in hyperplasia and dysplasia, and that invading cancer plays an important role in angiogenic switch. In the *MMP-$9^{-/-}$* nude mice used in our study, reduced tumorigenicity and angiogenesis were associated with inhibition of macrophage infiltration into lesions. Reconstitution of *MMP-$9^{+/+}$* cells in *MMP-$9^{-/-}$* nude mice by parabiosis was associated with infiltration of the tumors by MMP-9–expressing macrophages, enhanced angiogenesis, and progressive tumor growth. Activated macrophages can influence the angiogenic process by secreting enzymes that can break down the extracellular matrix and by secreting angiogenic molecules and growth factors, such as basic fibroblast growth factor, transforming growth factor α and β, insulin-like growth factor I, platelet-derived growth factor, and vascular endothelial growth factor/vascular permeable factor [38–40].

The number of macrophages that infiltrate tumors has been shown to directly correlate with MVD [34]. In clinical samples of human pancreatic tumors, MMP-9 is expressed in both epithelial and stromal cells [29,30]. Our finding that decreased angiogenesis of pancreatic tumors in *MMP-$9^{-/-}$* nude mice was associated with a decrease in macrophage infiltration into the tumors supports the conclusion that macrophages positively influence the vascularization of human pancreatic tumors. To infiltrate a tissue, macrophages must penetrate the extracellular matrix. Our data provide direct evidence that MMP-9 is involved in this process. Consistent with the decrease in macrophage infiltration into tumors growing in MMP-$9^{-/-}$ nude mice, parabiosed macrophages from MMP-$9^{-/-}$ nude mice were less capable of

penetrating a reconstituted extracellular matrix than were those from *MMP-9*$^{+/+}$ nude mice. Whether these data are applicable to other infiltrating cells (e.g., neutrophils) is unclear [41–43].

In summary, we have demonstrated that macrophage-derived MMP-9 contributes to the angiogenesis and growth of human pancreatic cancers implanted in the pancreas of nude mice. Our data do not exclude the possibility that other host cells, such as endothelial cells, mast cells, and neutrophils, could have contributed MMP-9 [2,3,24,43,44]. In any event, we found that deficiency of MMP-9 in host cells (but not in tumor cells) inhibited neoplastic angiogenesis and, hence, the growth of human pancreatic cancer cells in the pancreas of nude mice. Targeting the expression of MMP-9 in tumor cells and, more importantly, in specific host cells may therefore be an effective approach to controlling the angiogenesis and growth of pancreatic tumors.

Acknowledgements

The authors thank Dawn Chalaire for critical editorial comments and Lola López for expert preparation of this manuscript.

References

[1] Fidler IJ (2003). The pathogenesis of cancer metastasis: the 'seed and soil' hypothesis revisited (Timeline). *Nat Rev Cancer* **3**, 453–458.

[2] Folkman J (1992). The role of angiogenesis in tumor growth. *Semin Cancer Biol* **3**, 65–71.

[3] Coussens LM and Werb Z (2002). Inflammation and cancer. *Nature* **420**, 860–867.

[4] Coussens LM and Werb Z (2001). Inflammatory cells and cancer: think different! *J Exp Med* **193**, F23–F26.

[5] Lin EY and Pollard JW (2004). Role of infiltrated leucocytes in tumour growth and spread. *Br J Cancer* **90**, 2053–2058.

[6] Shimura S, Yang G, Ebara S, Wheeler TM, Frolov A, and Thompson TC (2000). Reduced infiltration of tumor-associated macrophages in human prostate cancer: association with cancer progression. *Cancer Res* **60**, 5857–5861.

[7] Cho Y, Miyamoto M, Kato K, Fukunaga A, Shichinohe T, Kawarada Y, Hida Y, Oshikiri T, Kurokawa T, Suzuoki M, et al. (2003). $CD4^+$ and $CD8^+$ T cells cooperate to improve prognosis of patients with esophageal squamous cell carcinoma. *Cancer Res* **63**, 1555–1559.

[8] Welsh TJ, Green RH, Richardson D, Waller DA, O'Byrne KJ, and Bradding P (2005). Macrophage and mast-cell invasion of tumor cell islets confers a marked survival advantage in non–small-cell lung cancer. *J Clin Oncol* **23**, 8959–8967.

[9] Tan SY, Fan Y, Luo HS, Shen ZX, Guo Y, and Zhao LJ (2005). Prognostic significance of cell infiltrations of immunosurveillance in colorectal cancer. *World J Gastroenterol* **11**, 1210–1214.

[10] Bates GJ, Fox SB, Han C, Leek RD, Garcia JF, Harrius AL, and Banham AH (2006). Quantification of regulatory T cells enables the identification of high-risk breast cancer patients and those at risk of late relapse. *J Clin Oncol* **24**, 5373–5380.

[11] Fukunaga A, Miyamoto M, Cho Y, Murakami S, Kawarada Y, Oshikiri T, Kato K, Kurokawa T, Suzuoki M, Nakakubo Y, et al. (2004). $CD8^+$ tumor-infiltrating lymphocytes together with $CD4^+$ tumor-infiltrating lymphocytes and dendritic cells improve the prognosis of patients with pancreatic adenocarcinoma. *Pancreas* **28**, 26–31.

[12] Jamieson NB, Glen P, McMillan DC, McKay CJ, Foulis AK, Carter R, and Imrie CW (2005). Systemic inflammatory response predicts outcome in patients undergoing resection for ductal adenocarcinoma head of pancreas. *Br J Cancer* **92**, 21–23.

[13] Hiraoka N, Onozato K, Kosuge T, and Hirohashi S (2006). Prevalence of $FOXP3^+$ regulatory T cells increases during the progression of pancreatic ductal adenocarcinoma and its premalignant lesions. *Clin Cancer Res* **12**, 5423–5434.

[14] Howes N and Neoptolemos JP (2002). Risk of pancreatic ductal adenocarcinoma in chronic pancreatitis. *Gut* **51**, 765–766.

[15] Lowenfels AB, Maisonneuve P, Cavallini G, Ammann RW, Lankisch PG, Andersen JR, Dimagno EP, Andrén-Sandberg A, and Domellöf L (1993). Pancreatitis and the risk of pancreatic cancer. International Pancreatitis Study Group. *N Engl J Med* **328**, 1433–1437.

[16] Otsuki M (2003). Chronic pancreatitis in Japan: epidemiology, prognosis, diagnostic criteria, and future problems. *J Gastroenterol* **38**, 315–326.

[17] Iacobuzio-Donahue CA, Ryu B, Hruban RH, and Kern SE (2002). Exploring the host desmoplastic response to pancreatic carcinoma: gene expression of stromal and neoplastic cells at the site of primary invasion. *Am J Pathol* **160**, 91–99.

[18] Farrow B, Sugiyama Y, Chen A, Uffort E, Nealon W, and Mark Evers B (2004). Inflammatory mechanisms contributing to pancreatic cancer development. *Ann Surg* **239**, 763–769.

[19] Esposito I, Menicagli M, Funel N, Bergmann F, Boggi U, Mosca F, Bevilacqua G, and Campani D (2004). Inflammatory cells contribute to the generation of an angiogenic phenotype in pancreatic ductal adenocarcinoma. *J Clin Pathol* **57**, 630–636.

[20] de Visser KE, Korets LV, and Coussens LM (2005). *De novo* carcinogenesis promoted by chronic inflammation is B lymphocyte dependent. *Cancer Cell* **7**, 411–423.

[21] Fidler IJ and Ellis LM (1994). The implications of angiogenesis for the biology and therapy of cancer metastasis. *Cell* **79**, 185–188.

[22] Liotta LA, Steeg PS, and Stetler-Stevenson WG (1991). Cancer metastasis and angiogenesis: an imbalance of positive and negative regulation. *Cell* **64**, 327–336.

[23] Aznavoorian S, Murphy AN, Stetler-Stevenson WG, and Liotta LA (1993). Molecular aspects of tumor cell invasion and metastasis. *Cancer* **71**, 1368–1383.

[24] Coussens LM, Tinkle CL, Hanahan D, and Werb Z (2000). MMP-9 supplied by bone marrow–derived cells contributes to skin carcinogenesis. *Cell* **103**, 481–490.

[25] Bergers G, Brekken R, McMahon G, Vu TH, Itoh T, Tamaki K, Tanzawa K, Thorpe P, Itohara S, Werb Z, et al. (2000). Matrix metalloproteinase-9 triggers the angiogenic switch during carcinogenesis. *Nat Cell Biol* **2**, 737–744.

[26] Itoh T, Tanioka M, Yoshida H, Yoshioka T, Nishimoto H, and Itohara S (1998). Reduced angiogenesis and tumor progression in gelatinase A–deficient mice. *Cancer Res* **58**, 1048–1051.

[27] Vu TH, Shipley JM, Bergers G, Berger JE, Helms JA, Hanahan I, Shapiro SD, Senior RM, and Werb Z (1998). MMP-9/gelatinase B is a key regulator of growth plate angiogenesis and apoptosis of hypertrophic chondrocytes. *Cell* **93**, 411–412.

[28] Huang S, Van Arsdall M, Tedjarati S, McCarty M, Wu W, Langley R, and Fidler IJ (2002). Contributions of stromal metalloproteinase-9 to angiogenesis and growth of human ovarian carcinoma in mice. *J Natl Cancer Inst* **94**, 1134–1142.

[29] Gress TM, Müller-Pillasch F, Lerch MM, Friess H, Büchler M, and Adler G (1995). Expression and *in-situ* localization of genes coding for extracellular matrix proteins and extracellular matrix degrading proteases in pancreatic cancer. *Int J Cancer* **62**, 407–413.

[30] Kuniyasu H, Ellis LM, Evans DB, Abbruzzese JL, Fenogio CJ, Bucana CD, Cleary KR, Tahara E, and Fidler IJ (1999). Relative expression of E-cadherin and type IV collagenase genes predicts disease outcome in patients with resectable pancreatic carcinoma. *Clin Cancer Res* **5**, 25–33.

[31] Nagakawa Y, Aoki T, Kasuya K, Tsuchida A, and Koyanagi Y (2002). Histologic features of venous invasion, expression of vascular endothelial growth factor and matrix metalloproteinase-2 and matrix metalloproteinase-9, and the relation with liver metastasis in pancreatic cancer. *Pancreas* **24**, 169–178.

[32] Bruns CJ, Harbison MT, Kuniyasu H, Eue I, and Fidler IJ (1999). *In vivo* selection and characterization of metastatic variants from human pancreatic adenocarcinoma by using orthotopic implantation in nude mice. *Neoplasia* **1**, 50–62.

[33] Eichwald EJ, Lustgraaf EC, and Strainer M (1959). Genetic factors in parabiosis. *J Natl Cancer Inst* **23**, 1193–1213.

[34] Yoneda J, Kuniyasu H, Crispens MA, Price JE, Bucana CD, and Fidler IJ (1998). Expression of angiogenesis-related genes and progression of human ovarian carcinomas in nude mice. *J Natl Cancer Inst* **90**, 447–454.

[35] Eggan K, Jurga S, Gosden R, Min IM, and Wagers AJ (2006). Ovulated oocytes in adult mice derive from non-circulating germ cells. *Nature* **441**, 1109–1114.

[36] Polverini PJ and Leibovich JS (1984). Induction of neovascularization *in vivo* and endothelial proliferation *in vitro* by tumor-associated macrophages. *Lab Invest* **51**, 635–642.
[37] Coussens LM, Raymond WW, Bergers G, Laig-Webster M, Behrendtsen O, Werb Z, Caughey GH, and Hanahan D (1999). Inflammatory mast cells upregulate angiogenesis during squamous epithelial carcinogenesis. *Genes Dev* **13**, 1382–1397.
[38] Mantovani A, Bottazzi B, Colotta F, Sozzani S, and Ruco L (1992). The origin and function of tumor-associated macrophages. *Immunol Today* **13**, 265–270.
[39] Sunderkotter C, Steinbrink K, Goebeler M, Bhardwaj R, and Sorg C (1994). Macrophages and angiogenesis. *J Leukoc Biol* **55**, 410–422.
[40] Koch AE, Polverini PJ, Kunkel SL, Harlow LA, DiPietro LA, Elner VM, Elner SG, and Strieter RM (1992). Interleukin-8 as a macrophage-derived mediator of angiogenesis. *Science* **258**, 1798–1801.
[41] Betsuyaku T, Shipley JM, Liu Z, and Senior RM (1999). Neutrophil emigration in the lungs, peritoneum, and skin does not require gelatinase B. *Am J Respir Cell Mol Biol* **20**, 1303–1309.
[42] Liu Z, Shipley JM, Vu TH, Zhou X, Diaz LA, Werb Z, and Senior RM (1998). Gelatinase B–deficient mice are resistant to experimental bullous pemphigoid. *J Exp Med* **188**, 475–482.
[43] Nozawa H, Chiu C, and Hanahan D (2006). Infiltrating neutrophils mediate the initial angiogenic switch in a mouse model of multistage carcinogenesis. *Proc Natl Acad Sci USA* **103**, 12493–12498.
[44] Fidler IJ (1995). Modulation of the organ microenvironment for treatment of cancer metastasis. *J Natl Cancer Inst* **87**, 1588–1592.